Channel switching effect in photodissociating N_2O^+ ion at 312.5 nm

Haifeng Xu, Ying Guo, Qifeng Li, Yong Shi, Shilin Liu,[a] and Xingxiao Ma
Open Laboratory of Bond Selective Chemistry, Department of Chemical Physics, University of Science and Technology of China, Hefei, Anhui 230026, China

(Received 6 April 2004; accepted 20 May 2004)

A experimental observation is presented on the N_2O^+ photodissociation process, which exhibits a complete channel switching effect in a narrow energy range. The N_2O^+ ions, prepared at the $X\,^2\Pi$ (000) state by (3+1) multiphoton ionization of neutral N_2O molecules at 360.6 nm, were excited to different vibrational levels in the $A\,^2\Sigma^+$ state in a wavelength range of 275–328 nm. Based on the estimates of total released kinetic energies from the time-of-flight mass spectrum, it was found that the dissociation pathway of $N_2O^+(A\,^2\Sigma^+)$, $NO^+(X\,^1\Sigma^+)+N(^4S)$ with lower dissociation limit, changes abruptly and completely to $NO^+(X\,^1\Sigma^+)+N(^2D)$ with higher dissociation limit, in a excitation energy range of merely 250 cm^{-1} at $\lambda\sim312.5$ nm. This phenomenon was explained by competition between the two dissociation pathways across the special excitation energy region.
 [DOI: 10.1063/1.1772363]

I. INTRODUCTION

The N_2O^+ molecular ion plays an important role in ionospheric chemistry, as it is the intermediate product in the reaction of O^+ and N_2.[1,2] Extensive spectroscopic studies have been performed to the electronic ground state $X\,^2\Pi$ and several lowest vibrational levels of the $A\,^2\Sigma^+$ state with many experimental methods, such as fluorescence emission spectrum,[3–7] fast ion beam laser spectroscopy (FIBLAS),[8,9] photoelectron spectroscopy,[10,11] and photoelectron-photoion coincidence (PEPICO) spectroscopy.[12] Recently, we extended the spectroscopic study of $N_2O^+(A\,^2\Sigma^+)$ to higher vibrational levels, and performed a systematic analysis on its photofragment excitation spectrum.[13] The spectral constants, such as vibrational frequencies, anharmonic constants, and Fermi interaction constant, were determined with relatively high reliability and precision due to the observation of many new vibrational levels in the $A\,^2\Sigma^+$ state.

The previous photodissociation studies of $N_2O^+(A\,^2\Sigma^+)$ were only limited to several lowest vibrational levels.[8,9,12] Photo-emission studies[3–7] showed that N_2O^+ ion at these lowest vibrational levels in the $A\,^2\Sigma^+$ state can fluoresce, and except for the ground vibrational levels, all the excited levels undergo a predissociation process to produce $N(^4S)$ and $NO^+(X\,^1\Sigma^+,v)$ fragments. It was known from the FIBLAS spectroscopic studies[8,9] that the population distribution of NO^+ fragment from the N_2O^+ dissociation at the $A\,^2\Sigma^+$ (100) level centers at $v=4$. Furthermore, the PEPICO study at the (100), (001), and (200) levels showed that NO^+ fragment populates mainly at $v=4$ or 5 level.[12] Interestingly, a quite different vibrational distribution of NO^+ was found from dissociation at the level (300),[12] which was interpreted by the formation of NO^+ populating at high vibrational levels, $v=8$ or 9, or by the opening of a new dissociation channel with higher limit, $NO^+(X\,^1\Sigma^+)+N(^2D)$, from which the NO^+ fragment populates at low vibrational levels, $v=0$ or 1. Unfortunately, due to the insufficient experimental data, the dominant dissociation channel could not be determined.

The dissociation of N_2O^+ at the lowest levels of the $A\,^2\Sigma^+$ state, has been known to be via the lower dissociation channel $NO^+(X\,^1\Sigma^+)+N(^4S)$. The mechanism has been investigated theoretically[14,15] and has been well established that the dissociation is a two-step process, i.e., the $A\,^2\Sigma^+$ state first couples with a bound $1\,^4\Pi$ state through spin-orbit interaction, and then couples to a dissociative $1\,^4\Sigma^-$ continuum, which finally leads to $NO^+(X\,^1\Sigma^+)$ and $N(^4S)$ fragments. The crossing of the $A\,^2\Sigma^+$ and $1\,^4\Pi$ states lies between the (000) and (100) vibrational levels of the $A\,^2\Sigma^+$ state, and therefore, makes all the vibrational levels predissociative, except for the (000) level.

Despite of extensive works regarding the dissociation at vibrational levels below (300) of the $A\,^2\Sigma^+$ state, there have been very few reports about dissociation at vibrational levels higher than the (300) level, and the dissociation mechanism is still unclear. In this work, we studied the photodissociation process of N_2O^+ ion at the $A\,^2\Sigma^+$ state, by preparing N_2O^+ at the $X\,^2\Pi$ (000) state and exciting it to different vibrational levels in the $A\,^2\Sigma^+$ state in a excitation energy range of 30 500 cm^{-1} to 36 000 cm^{-1}. From the analysis of the total released kinetic energies after dissociation, we found that the higher $NO^+(X\,^1\Sigma^+)+N(^2D)$ dissociation channel is opened abruptly at around 32 000 cm^{-1}, and replaces completely the already opened lower dissociation channel, $NO^+(X\,^1\Sigma^+)+N(^4S)$, by a mere $\sim$250 cm^{-1} excitation energy increase.

II. EXPERIMENT

The experimental setup has been described in detail elsewhere,[16] and is essentially similar to the spectroscopic experiment on $N_2O^+(A\,^2\Sigma^+)$.[13] Briefly, the N_2O^+ ions were prepared by (3+1) REMPI of supersonically jet-cooled N_2O molecules at 360.55 nm with a pulsed Nd:YAG laser pumped dye laser. This ionization laser, $\sim$2 mJ/pulse, was focused

[a]Author to whom correspondence should be addressed. Electronic mail: slliu@ustc.edu.cn

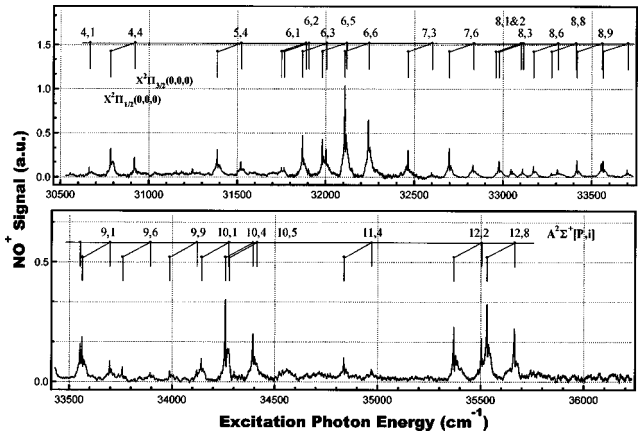

FIG. 1. The PHOFEX spectrum of N_2O^+ obtained by monitoring NO^+ fragment in the wavelength range of 275–328 nm, which is attributed to $A\,^2\Sigma^+ \leftarrow X\,^2\Pi_{(1/2,3/2)}\,(000)$ electronic transition and assigned in terms of cluster of vibrational levels coupled by Fermi-resonance in the $A\,^2\Sigma^+$ state. *P* and *i* in the figure represent the cluster dimension and the energy ordering number within the cluster increasing with energy, respectively. The spectrum here indicates that NO^+ is the dissociation product of N_2O^+ at the $A\,^2\Sigma^+$ state.

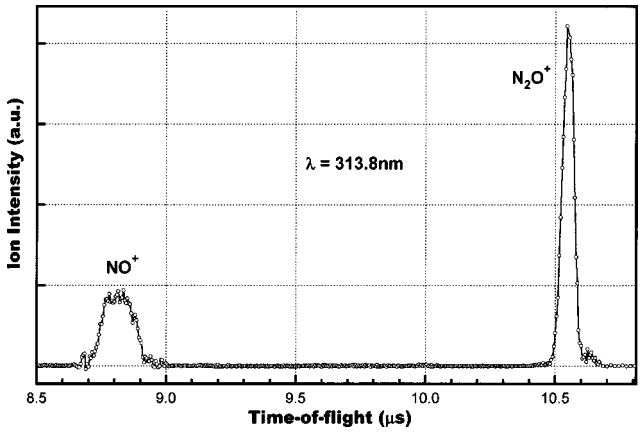

FIG. 2. A typical TOF mass spectrum measured at 313.8 nm. The width of NO^+ ion is much broader than that of the N_2O^+ parent ion, which is caused by the fragment recoil velocity distribution along the TOF axis after dissociation.

perpendicularly on the molecular beam by a quartz lens with $f=300$ mm. Under optimal conditions, pure N_2O^+ ions were generated without any obvious interference from fragment ions and lie at the vibrationless ground state, $X\,^2\Pi$ (000).[17,18] After a delay of 30 ns the resultant $N_2O^+(X\,^2\Pi)$ ions selectively prepared in this way were excited by another Nd:YAG laser pumped dye laser, ~1 mJ/pulse, to the dissociative $A\,^2\Sigma^+$ state in a wavelength range of 275–328 nm. The wavelength of this dissociation laser (bandwidth ~0.1 cm^{-1}) was calibrated simultaneously against the argon optogalvanic spectrum, resulting in an overall absolute uncertainty of ~0.5 cm^{-1} in the excitation energy. Both dye lasers counter propagated and spatially overlapped with each other. The parent N_2O^+ and photofragment ions were collected in a direction orthogonal to the laser beams and the molecular beams by a time-of-flight (TOF) mass spectrometer, and ion signals from the microchannel-plate detector were recorded with a digital oscilloscope (400 MHz) and processed by a boxcar integrator. The intensities of both lasers were monitored simultaneously during the experiment.

III. RESULTS AND DISCUSSIONS

A. Photofragment excitation (PHOFEX) spectrum

The predominant fragment ion in the studied wavelength range is NO^+, and very weak N_2^+ signal appears only at excitation wavelengths shorter than 282.7 nm (~35 370 cm^{-1}). These fragment ions were confirmed to be the dissociation products of parent N_2O^+ generated completely by the dissociation laser, by cutting off each of the two lasers, and by varying the temporal delay and the spatial overlap between the two lasers. By monitoring the NO^+ signal intensity and scanning the wavelength of the excitation laser, a photo-fragment excitation (PHOFEX) spectrum of N_2O^+ was obtained and shown in Fig. 1. This spectrum could be attributed completely to the $A\,^2\Sigma^+ \leftarrow X\,^2\Pi_{(1/2,3/2)}$ electronic transition of N_2O^+, and was assigned in terms of cluster of vibrational levels coupled by Fermi-resonance in the $A\,^2\Sigma^+$ state among zero-order vibrational levels, (V_1,V_2,V_3), (V_1-1,V_2+2,V_3), and (V_1-2,V_2,V_3+1). *P* in the figure represents the cluster dimension, $P=2V_1+V_2+4V_3$, and *i* the energy ordering number within the cluster increasing with the energy.[19] Detailed analysis has been published in this journal.[13] Here, the spectrum indicates that NO^+ fragment is the dissociation product of N_2O^+ $(A\,^2\Sigma^+)$.

As can be seen from Fig. 1 that the excitations of vibrational levels with odd *P*, i.e., zero-order vibrational levels with odd V_2, are observed. To the first-order approximation, the excitation of vibrational levels with odd quantum V_2 is forbidden in the linear-to-linear $A\,^2\Sigma^+ \leftarrow X\,^2\Pi$ (000) electronic transition. This should be caused by the vibronic interaction between the $A\,^2\Sigma^+$ and $X\,^2\Pi$ states, as stated by Dehmer *et al.*[10] As can be seen in Fig. 1, these forbidden bands are observed with considerable intensities despite their small Franck-Condon factors, and should be attributed to the high dissociation probabilities for these vibrational levels in the $A\,^2\Sigma^+$ state.

B. TOF profile analysis of NO^+ fragment

The TOF mass spectra were recorded at the peak positions of vibronic transition bands in the PHOFEX spectrum. Figure 2 shows a typical one at excitation/photolysis wavelength of 313.8 nm. It can be seen that the width of NO^+ fragment is much broader than that of the N_2O^+ parent ion. Since such a broadening is caused by the fragment recoil velocity along the TOF axis, the NO^+ speed distributions, and in turn the total released kinetic energies E_{total} at different photolysis wavelengths, can be roughly determined from the NO^+ TOF profiles.

Let Δt be the full-width at half-maximum of the NO^+ TOF profile and Δt_0 be the width of a Gaussian instrumental profile estimated from the TOF width of parent N_2O^+, the kinetic energy of NO^+ (and also E_{total}) should increase monotonically with $(\Delta t)^2-(\Delta t_0)^2$. More precisely, the total released kinetic energies E_{total} can be determined from the simulation of NO^+ TOF profile. Assuming the NO^+

fragment is created with a Gaussian-type kinetic energy distribution $P(E_{NO^+})$, and transferring $P(E_{NO^+})$ into the NO^+ speed distribution $g(V_{NO^+})$ by

$$g(V_{NO^+}) = P(E_{NO^+})(dE_{NO^+}/dV_{NO^+}), \quad (1)$$

the recoil velocity distribution of NO^+ along the TOF axis, $f(V_z)$, at the "*magic angle*" (the angle between the TOF axis and the photolysis laser polarization, 54.7°), is expressed as the projection of the NO^+ speed distribution $g(V_{NO^+})$ onto the TOF axis,[20]

$$f(V_z) = \int_{|V_z|}^{\infty} \frac{g(V_{NO^+})}{2V_{NO^+}} dV_{NO^+}. \quad (2)$$

In the absence of TOF instrumental effect, the distribution $f(V_z)$ is directly related to the flight time distribution $h(t-t_0)$ by

$$h(t-t_0) = \frac{qE}{m} f(V_z), \quad (3)$$

where m, q, and E represent the mass of NO^+, the ion charge and the electric intensity of the TOF extraction field, respectively. Therefore, the experimentally observed TOF profile $G(t)$ of NO^+ fragment is the distribution $h(t\text{-}t_0)$ convoluted by a Gaussian instrumental profile $I(t)$, which can be determined from the TOF profile of parent N_2O^+ ion,

$$G(t) = \int_{-\infty}^{\infty} h(t-t_0-t')I(t')dt'. \quad (4)$$

Using Eqs. (1)–(4), the NO^+ TOF profile could be simulated, and the speed distribution $g(V_{NO^+})$ could be then determined.

With the determined $g(V_{NO^+})$, the total released kinetic energy distribution $P(E_{total})$ can be obtained according to the momentum conservation during the dissociation using the following relations:

$$E_{total} = \frac{1}{2}\left(\frac{Mm}{M-m}\right) v_{NO^+}^2,$$

$$P(E_{total}) = \frac{g(v_{NO^+})}{v_{NO^+}}\left(\frac{M-m}{Mm}\right), \quad (5)$$

where M is the mass of N_2O^+ parent ion. From the distribution $P(E_{total})$, the averaged total kinetic energy, $\langle E_{total}\rangle$, could be determined.

Figure 3(a) shows the NO^+ TOF profile at $\lambda = 313.8$ nm obtained at the magic angle and its simulation (the periodic oscillations in the figure are due to the electric noise in our experiment). As a comparison, Fig. 3(b) shows the NO^+ TOF profile at $\lambda = 311.4$ nm. It can be seen clearly that the TOF width at 311.4 nm is much narrower than that at 313.8 nm, although the difference of excitation photon energy is merely 245 cm^{-1}. As will be seen in the following section, this is due to the dissociation channel switching effect of N_2O^+ occurring in this region.

C. Dissociation channel switching effect

The total released kinetic energies $\langle E_{total}\rangle$ determined from the NO^+ TOF simulations at different excitation wavelengths, as well as the values of $(\Delta t)^2-(\Delta t_0)^2$, are illustrated in Fig. 4 as a function of the photo-excitation energy. It can be seen that both $(\Delta t)^2-(\Delta t_0)^2$ and $\langle E_{total}\rangle$ vary in a very similar way with the excitation energy, confirming the reliability of our determined $\langle E_{total}\rangle$. At excitation energies below 32 000 cm^{-1}, $\langle E_{total}\rangle$s are around 8 000 cm^{-1}, which are quite consistent with previous results at the (100) level of N_2O^+ ($A\,^2\Sigma^+$).[8,9]

It is interesting to note that, at excitation energy around 32 000 cm^{-1} ($\lambda \sim 312.5$ nm), $\langle E_{total}\rangle$ decreases abruptly from $\sim$8000 cm^{-1} to $\sim$1600 cm^{-1} in a excitation energy range of $\sim$250 cm^{-1}. With further increase of the excitation energy, $\langle E_{total}\rangle$ increases almost linearly from 1600 cm^{-1} to 4 000

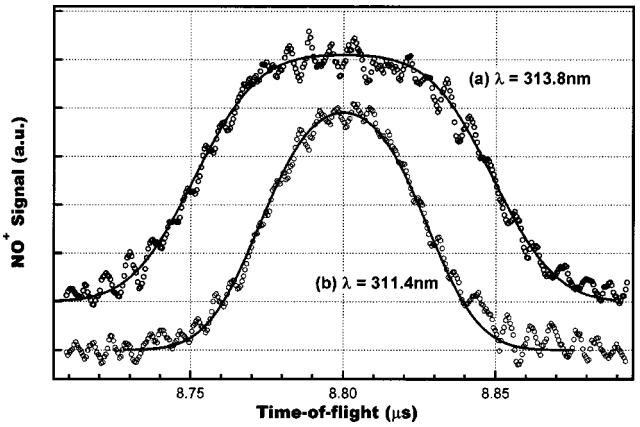

FIG. 3. (a) The observed TOF profile of NO^+ (circle) measured at magic angle (54.7°) relative to the laser polarization at $\lambda = 313.8$ nm, and its simulation (solid line) by assuming NO^+ is created with a Gaussian-type kinetic energy distribution and by convoluting the corresponding velocity projection along the TOF axis with a Gaussian instrumental profile of width 30 ns. (b) the observed TOF profile of NO^+ (circle) at $\lambda = 311.4$ nm and its simulation (solid line). Although the excitation difference is merely 250 cm^{-1} between (a) and (b), the TOF width at 311.4 nm is much narrower than that at 313.8 nm, which is due to the dissociation channel switching effect of N_2O^+ occurring in this excitation region.

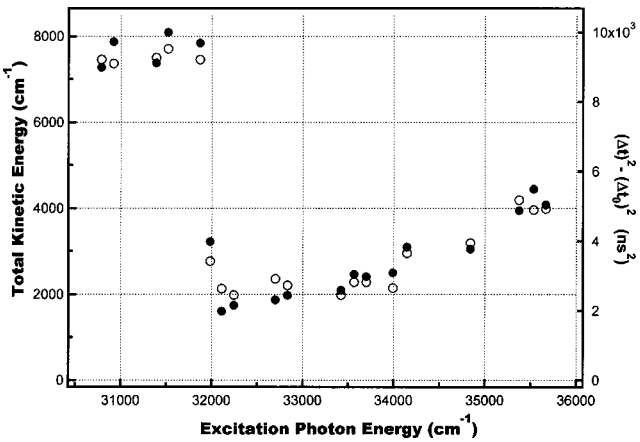

FIG. 4. Variation of total released kinetic energy (solid circle) with the excitation photon energy determined from the simulation of NO^+ TOF profile, and the net TOF broadening $(\Delta t)^2-(\Delta t_0)^2$ (opened circle) caused by its recoil velocity along the TOF axis. Δt represents the width of TOF profile, and Δt_0 the width of instrumental profile. The abrupt and deep decrease of total kinetic energy at $\sim$32 000 cm^{-1} indicates that a new dissociation channel is opened and plays a dominant role in a narrow excitation energy region.

cm^{-1} at excitation energy of 35 500 cm^{-1}. Such a sudden drop in $\langle E_{total}\rangle$ can not be attributed to the increase of NO^+ internal energy. Since the vibrational frequency of $NO^+(X\,^1\Sigma^+)$ is 2 376 cm^{-1} and energy gap between the lowest electronically excited state and the $X\,^1\Sigma^+$ state is 52 190 cm^{-1}, the 6 400 cm^{-1} decrease in $\langle E_{total}\rangle$ implies an increase of 2–3 vibrational quantum numbers of NO^+ $(X\,^1\Sigma^+)$. It is unlikely that such an abrupt change occurs in an excitation energy range of merely 250 cm^{-1}. The only possibility is that a new dissociation channel with a higher limit has been opened suddenly and becomes the main dissociation pathway.

It is known that there are two dissociation limits to produce NO^+ fragment in the present studied wavelength range, i.e., $NO^+(X\,^1\Sigma^+)+N(^4S)$ at 10 430 cm^{-1} (Channel A), and $NO^+(X\,^1\Sigma^+)+N(^2D)$ at 29 660 cm^{-1} (Channel B).[3] Therefore, the already opened channel at low excitation energy region should be Channel A, and the newly opened channel at around 32 000 cm^{-1} should be Channel B. Since the dissociation limit of Channel B is much higher than that of Channel A, as long as Channel B is opened, the total released kinetic energy from this channel will decrease remarkably, causing the decrease of measured $\langle E_{total}\rangle$. Furthermore, the decrease of $\langle E_{total}\rangle$ from ~8000 cm^{-1} to ~1600 cm^{-1} indicates that the contribution of Channel A should not exceed 20%, meaning that Channel B replaces Channel A and becomes the main dissociation pathway. Further analysis will show that the dissociation pathway changes completely from Channel A to Channel B at excitation energy around 32 000 cm^{-1}.

With the determined $\langle E_{total}\rangle$s at excitation energies below 32 000 cm^{-1}, the partition ratio of total released kinetic energy in total available excess energy ($E_{avl}=h\nu-10\,430\,cm^{-1}$) for Channel A, $P_A=\langle E_{total}\rangle/E_{avl}$, was estimated to be around 37%. It is reasonable to assume that for each of the two dissociation pathways the corresponding kinetic energy partition ratio remains unchanged with excitation energy. The measured total kinetic energies in the excitation energy range from 32 000 cm^{-1} to 35 500 cm^{-1} should be the contributions of the two channels, which can be expressed as

$$\langle E_{total}\rangle=(h\nu-10\,430)P_A(1-C_B)+(h\nu-29\,660)P_BC_B, \quad (6)$$

where C_B and P_B are the fraction and the kinetic energy partition ratio of Channel B, respectively. From the measured values of $\langle E_{total}\rangle$ in this excitation energy region, P_B was determined to be 68%, and C_B was found to be close to unity. This implies that at excitation energies above 32 000 cm^{-1} the only dissociation pathway of $N_2O^+(A\,^2\Sigma^+)$ is Channel B, and that Channels A switches to Channel B at around 32 000 cm^{-1}. The dissociation channel switching process occurs in an excitation energy range of ~250 cm^{-1}.

D. Predissociation mechanism

This switching effect was attributed to the competition between the two dissociation channels. All previous works regarding the dissociation mechanism concentrated mainly at low excitation energy regions corresponding to dissociation Channel A. The dissociation mechanism for Channel A has been well established by previous theoretical studies.[14,15] The $A\,^2\Sigma^+$ state first couples with the bound $1\,^4\Pi$ state via spin-orbit interaction, the latter couples to the repulsive $1\,^4\Sigma^-$ state, and finally leads to $NO^+(X\,^1\Sigma^+)$ and $N(^4S)$ fragments. Therefore, the dissociation rate is governed by the weak spin-orbit coupling strength between the $A\,^2\Sigma^+$ and the $1\,^4\Pi$ states. For the dissociation Channel B, since it correlates to the adiabatic dissociation limit of the ground state $X\,^2\Pi$ of N_2O^+,[10] it must originate from the dissociation in the $X\,^2\Pi$ state. As indicated by Dehmer *et al.*[10] and Chen *et al.*,[11] and also as shown in our spectroscopic study of $N_2O^+(A\,^2\Sigma^+)$,[13] the $A\,^2\Sigma^+$ state can also interact with the $X\,^2\Pi$ state via vibronic coupling, although this interaction can not lead to the dissociation via Channel B in previously studied low excitation energy range. But if energetically allowed, the $A\,^2\Sigma^+$ state would dissociate due to the coupling with the $X\,^2\Pi$ state, leading to the dissociation via Channel B.

In linear geometries, since the $A\,^2\Sigma^+$ and $X\,^2\Pi$ states differ by one spin orbital, and their vibronic coupling strength would be distinctly larger than that between the $A\,^2\Sigma^+$ and $1\,^4\Pi$ states, which differs by two spin orbitals. Therefore, if energetically allowed, the dissociation rate from the $X\,^2\Pi$ state (Channel B) should be much larger than that from the $1\,^4\Pi$ and $1\,^4\Sigma^-$ states (Channel A). This means that dissociation from Channel B should be much more competitive than that from Channel A, and that Channel B should replace Channel A to become the dominant dissociation pathway. In fact, from the above analyses of the TOF profiles, it is found that Channel A switches completely to Channel B at excitation energies above 32 000 cm^{-1}. Since for the dissociation Channel B, $N_2O^+(A\,^2\Sigma^+)$ has less time to redistribute its total available excess energy among the internal degrees, the kinetic energy partition ratio must be larger than that for Channel A, as confirmed from our analyses. Our observed dissociation channel switching position (~32 000 cm^{-1}) is roughly 2 340 cm^{-1} higher than the threshold energy of Channel B. This could be attributed to the existence of a potential barrier along the N—NO^+ bond stretching at the $X\,^2\Pi$ state, as predicted by Chambaud *et al.*[15]

Besides the predominant fragment ion NO^+, we also observed another weak fragment ion N_2^+ from $N_2O^+(A\,^2\Sigma^+)$ dissociation at excitation energies above 35 370 cm^{-1}. The observed appearance threshold of N_2^+, 35 370 cm^{-1}, is quite close to the limit of the dissociation channel $N_2^+(X\,^2\Sigma_g^+)+O(^3P_2)$ (35 140 cm^{-1}).[3] Since this channel also correlates to the adiabatic dissociation from the $X\,^2\Pi$ state,[10] it should be the dissociation production at the $A\,^2\Sigma^+$ state via the vibronic coupling with the $X\,^2\Pi$ state, which is similar to the dissociation Channel B.

IV. CONCLUSION

In the present study, the dissociation process of N_2O^+ at the $A\,^2\Sigma^+$ state in the energy range of 30 500–36 000 cm^{-1} has been investigated. By simulating the TOF profiles of NO^+ fragment, the total released kinetic energies $\langle E_{total}\rangle$ at

different excitation wavelengths were roughly determined. $\langle E_{\text{total}} \rangle$ is about 8 000 cm^{-1} at lower excitation energies, drops abruptly to 1 600 cm^{-1} at around 32 000 cm^{-1}, and increases gradually with excitation energy above 32 000 cm^{-1}. Analysis showed that at energies below $\sim$32 000 cm^{-1} the dissociation pathway is $NO^+(X\,^1\Sigma^+) + N(^4S)$ (Channels A), and at energies above $\sim$32 000 cm^{-1} the dissociation pathway is $NO^+(X\,^1\Sigma^+) + N(^2D)$ (Channel B). Channel A switches completely to Channel B at $\sim$32 000 cm^{-1} in an excitation energy range of merely $\sim$250 cm^{-1}.

The dissociation mechanism for both channels is discussed based on the experimental results. The dissociation via Channel A is indirect, the $A\,^2\Sigma^+$ state is slowly predissociated by a bound $1\,^4\Pi$ state as intermediate state via spin-orbit coupling, the latter is then coupled to a repulsive $1\,^4\Sigma^-$ state. The dissociation via Channel B is caused by the vibronic coupling between the $A\,^2\Sigma^+$ state and the $X\,^2\Pi$ state. The dissociation channel switching is attributed to the overwhelming dissociation rate via the $A\,^2\Sigma^+/X\,^2\Pi$ coupling over that via the $A\,^2\Sigma^+/1\,^4\Pi$ interaction at energies necessary for the opening of Channel B.

ACKNOWLEDGMENTS

The present work was supported financially by the National Natural Science Foundation of China (Grant No. 20273063), and the NKBRSF research program (Grant No. G1999075304).

[1] J. D. Burley, K. M. Evin, and P. B. Armentrout, J. Chem. Phys. **86**, 1944 (1987).
[2] N. Komiha, J. Mol. Struct. **306**, 313 (1994).
[3] J. H. Callomon and F. Creutzberg, Philos. Trans. R. Soc. London, Ser. A **277**, 157 (1974).
[4] T. Ibuki and N. Sugita, J. Chem. Phys. **80**, 4625 (1984).
[5] M. Tsuji and J. Maier, Chem. Phys. **126**, 435 (1988).
[6] T. Imamura, T. Imajo, and I. Koyano, J. Phys. Chem. **99**, 15465 (1995).
[7] C. E. Fellows and M. Vervloet, Chem. Phys. **264**, 203 (2001).
[8] S. Abed, M. Broyer, M. Carre, M. L. Gaillard, and M. Larzilliere, Chem. Phys. **74**, 97 (1983).
[9] J. Lerme, S. Abed, M. Larzilliere, R. A. Holt, and M. Carre, J. Chem. Phys. **84**, 2167 (1986).
[10] P. M. Dehmer, J. L. Dehmer, and W. A. Chupka, J. Chem. Phys. **73**, 126 (1980).
[11] W. Chen, J. Liu, and C. Y. Ng, J. Phys. Chem. A **107**, 8086 (2003).
[12] M. Richard-Viard, O. Atabek, O. Dutuit, and P. M. Guyon, J. Chem. Phys. **93**, 8881 (1990).
[13] H. Xu, Y. Guo, Q. Li, S. Liu, X. Ma, J. Liang, and H. Li, J. Chem. Phys. **119**, 11609 (2003).
[14] J. A. Beswick and M. Horani, Chem. Phys. Lett. **78**, 4 (1981).
[15] G. Chambaud *et al.*, Mol. Phys. **98**, 1793 (2000).
[16] L. Zhang, J. Chen, H. Xu, J. Dai, S. Liu, and X. Ma, J. Chem. Phys. **114**, 10768 (2001).
[17] M. G. Szarka and S. C. Wallace, J. Chem. Phys. **95**, 2336 (1991).
[18] C. R. Scheper, J. Kuijt, W. J. Buma, and C. A. deLange, J. Chem. Phys. **109**, 7844 (1998).
[19] J. L. Teffo, V. I. Perevalov, and O. M. Lyulin, J. Mol. Spectrosc. **168**, 390 (1994).
[20] R. Vasudev, R. N. Zare, and R. N. Dixon, J. Chem. Phys. **80**, 4863 (1984).